

Hagedorn divergences and tachyon potential

Mauro Brigante¹, Guido Festuccia¹ and Hong Liu^{1,2}

¹ *Center for Theoretical Physics
Massachusetts Institute of Technology
Cambridge, Massachusetts, 02139*

² *Kavli Institute for Theoretical Physics
University of California
Santa Barbara, CA 93106-4030*

We consider the critical behavior for a string theory near the Hagedorn temperature. We use the factorization of the worldsheet to isolate the Hagedorn divergences at all genera. We show that the Hagedorn divergences can be resummed by introducing double scaling limits, which smooth the divergences. The double scaling limits also allow one to extract the effective potential for the thermal scalar. For a string theory in an asymptotic anti-de Sitter (AdS) spacetime, the AdS/CFT correspondence implies that the critical Hagedorn behavior and the relation with the effective potential should also arise from the boundary Yang-Mills theory. We show that this is indeed the case. In particular we find that the free energy of a Yang-Mills theory contains “vortex” contributions at finite temperature. Yang-Mills Feynman diagrams with vortices can be identified with contributions from boundaries of moduli space on the string theory side.

1. Introduction

Since the early days of string theory, it was observed that the free string spectrum has a density of states which grows exponentially with energy, and that the partition function $Z = e^{-\beta H}$ of a free string gas at a temperature $T = \frac{1}{\beta}$ would diverge when T is greater than some critical value T_H [1,2,3]. The Hagedorn divergence occurs for all known (super)string theories with spacetime dimensions greater than two. The physical meaning of the critical temperature T_H and of the divergence has been a source of much discussion since then.

In the late eighties, a few important observations were made which suggested that the Hagedorn divergence signals a phase transition, analogous to the deconfinement transition in QCD [4,5,6,7]. At the Hagedorn temperature T_H the lowest winding modes (with winding ± 1) around the periodic Euclidean time direction become marginal operators in the worldsheet conformal field theory [4,5,6]. Sathiapalan and Kogan [4,5] argued that above the Hagedorn temperature, the winding modes would condense in a fashion similar to the Kosterlitz-Thouless transition in the X-Y model and the worldsheet theory will flow to a new infrared fixed point. From the spacetime point of view, these winding modes (with winding ± 1) correspond to a complex scalar field ϕ living in one fewer spacetime dimension (i.e. not including Euclidean time). Near the Hagedorn temperature, the spacetime effective potential for ϕ can be written in a form

$$V = m_\phi^2(\beta)\phi^*\phi + \lambda_4 g_s^2(\phi^*\phi)^2 + \lambda_6 g_s^4(\phi^*\phi)^3 + \dots, \quad m_\phi^2(\beta) \propto T_H - T. \quad (1.1)$$

If λ_4 is positive (negative), the phase transition would be second order (first order). In [7] Atick and Witten argued that for a string theory in asymptotic flat spacetime the transition should be first order¹ (i.e. $\lambda_4 < 0$) due to the coupling of the thermal scalar to the dilaton.

While the one-loop Hagedorn divergence has been extensively discussed in the past (see e.g. [9,10] for reviews), Hagedorn divergences from higher genus amplitudes have been investigated rather little. In this paper we use a factorization argument to extract Hagedorn divergences for higher genus amplitudes. We show that they can be resummed by introducing various double scaling limits, which smooth the divergences. The double scaling limits also allow one to extract the effective potential (1.1) to arbitrary high orders. That a double scaling limits might exist for higher genus Hagedorn divergences was speculated earlier in [11] and further discussed in [12] in a toy model motivated from AdS/CFT.

¹ That the transition is of first order can also be argued from the non-perturbative instability of the thermal flat spacetime discovered in [8].

Our discussion further highlights that Hagedorn divergences signal a breakdown of string perturbation theory due to appearance of massless modes and do not imply a limiting temperature for string theory [4,5,7].

The discussion of this paper will be rather general, e.g. applicable to string theories in asymptotic anti-de Sitter (AdS) spacetime. The AdS/CFT correspondence then implies that the critical Hagedorn behavior from high genera and the relation with the effective potential should also arise from Yang-Mills theories. We show that this is indeed the case. In particular we find that the free energy of Yang-Mills theory contains “vortex” contributions at finite temperature. Yang-Mills Feynman diagrams with vortices can be identified with contributions from the boundary of the moduli space on the string theory side.

The plan of the paper is as follows. In section 2 we first review the one-loop result and discuss the physical set-up of our calculation. We then extract the critical Hagedorn behavior from higher genus amplitudes and show that one can find terms in (1.1) by defining suitable double scaling limits. In section 3 we turn to Yang-Mills theory. We discuss the structure of the large N expansion for the partition function of a Yang-Mills theory at finite temperature and isolate the critical Hagedorn behavior. We conclude in section 4 with a discussion of some physical implications.

2. High-loop Hagedorn divergences in perturbative string theory

2.1. Review of one-loop divergence and set-up

Consider a string theory consisting of a compact CFT times $\mathbb{R}^{1,d}$. The one-loop free energy of the system at a finite temperature can be computed by the torus path integral with a target space in which the Euclidean time direction is compactified with period $\beta = \frac{1}{T}$ and with anti-periodic boundary condition for spacetime fermions [13]. The Hagedorn singularity appears when the lowest modes with winding ± 1 around the compactified time direction become massless [6,4,5]. More explicitly, the mass square can be written as

$$m_\phi^2(\beta) = \left(\frac{\beta}{2\pi\alpha'}\right)^2 - c_0 \equiv \left(\frac{\beta}{2\pi\alpha'}\right)^2 - \left(\frac{\beta_H}{2\pi\alpha'}\right)^2 \quad (2.1)$$

where the first term is the winding contribution and c_0 is the zero point energy of the string (in the winding sector). The second equality of (2.1) should be considered as a definition of the Hagedorn temperature. From (2.1), $m_\phi^2(\beta) \rightarrow 0$ as $\beta \rightarrow \beta_H$ and becomes

tachyonic when $\beta < \beta_H$. In spacetime, the winding ± 1 modes correspond to a complex scalar field ϕ living in one fewer spacetime dimension (i.e. spatial part of the spacetime), which is often called the thermal scalar in the literature. We will follow this terminology below. We will also collectively call modes with general winding numbers (and no internal excitations) winding tachyons. Equation (2.1) applies to both bosonic and superstring theories with possibly different c_0 for different theories.

The critical behavior of the one-loop free energy F_1 as $\beta \rightarrow \beta_H$ is controlled by that of the thermal scalar

$$F_1 = -2 \times \frac{1}{2} \log(-\nabla^2 + m_\phi^2(\beta)) + F_{finite}, \quad \beta \rightarrow \beta_H \quad (2.2)$$

where ∇^2 is the Laplacian on the *spatial* manifold. If the gap of ∇^2 along the compact CFT directions is bigger than $m_\phi^2(\beta)$, the singular part of (2.2) can be further written as

$$\begin{aligned} F_1 &\propto - \int \frac{d^d k}{(2\pi)^d} \log(k^2 + m_\phi^2(\beta)) + \dots \\ &\propto \begin{cases} (m_\phi^2(\beta))^{\frac{d}{2}} & d \text{ odd} \\ (m_\phi^2(\beta))^{\frac{d}{2}} \log m_\phi^2(\beta) & d \text{ even} \end{cases} \end{aligned} \quad (2.3)$$

F_1 has a branch point singularity at $m_\phi^2(\beta) = 0$ for all d . In particular, for $d = 0$ it is logarithmically *divergent* as $\beta \rightarrow \beta_H$

$$F_1 = -\log(\beta - \beta_H) + \text{finite} . \quad (2.4)$$

The above discussion should also apply to a static curved spacetime, for example, an AdS spacetime, even though an explicit computation of the one-loop free energy is often not possible. For an AdS spacetime, since the Laplacian has a mass gap, we expect the free energy for a thermal gas of AdS strings should behave as (2.4) when the Hagedorn temperature is approached (see e.g. [14] for further discussion).

In this paper we will focus our discussion on $d = 0$ or more generally those spacetimes (including AdS) in which (2.4) is satisfied, for the following reasons:

1. The thermal ensemble cannot be defined in an uncompact asymptotically flat spacetime due to Jeans instability. To make the canonical ensemble well defined, an Infrared (IR) cutoff is needed. One particularly convenient (and well-defined) IR regulator is

to introduce a small negative cosmological constant². For our discussion below the precise nature of such a regulator will not be important as far as it makes the thermal ensemble well defined. Such IR regulators introduce a gap in the Laplacian ∇^2 , which will be kept fixed in the limit $T \rightarrow T_H$ and thus will be greater than m_ϕ^2 when the temperature is sufficiently close to T_H .

2. The Hagedorn singularity is sharpest at $d = 0$. While the free energy is singular at $\beta = \beta_H$ for all dimensions, it is divergent only for $d = 0$.

The logarithmic divergence of (2.4) at $\beta \rightarrow \beta_H$ implies that the string perturbation theory breaks down *before* $\beta = \beta_H$ is reached. Thus it is not sufficient to consider only the one-loop contribution to the free energy and higher genus contributions could be important. Below we will show that as $\beta \rightarrow \beta_H$, it is necessary to resum the string perturbation theory to all orders. We will then show that one can extract the spacetime effective action for the thermal scalar from the resummed series and that the divergences are smoothed out.

When λ_4 in (1.1) is negative, i.e. when the transition is first order, there exists a lower temperature $T_c < T_H$, at which the thermal gas of strings becomes metastable. At a temperature $T_c < T < T_H$, the thermal gas is still perturbatively stable. Here we are interested in probing the critical behavior in the metastable phase (or superheated phase) as $T \rightarrow T_H$ from below.

2.2. Higher loop divergences

We now examine higher loop divergences as $\beta \rightarrow \beta_H$. For simplicity we will restrict our discussion to bosonic strings. We expect the conclusion to hold for superstring theories as well.

² In an asymptotic AdS spacetime it is possible to define a canonical ensemble in the presence of gravity, as discovered by Hawking and Page [15]. Hawking and Page also found that the system undergoes a first order phase transition at a temperature T_{HP} from a thermal gas in AdS to a stable black hole. Treating an AdS spacetime with a small cosmological constant as an IR regularization of the flat spacetime, it is natural to identify the first order phase transition argued by [7] with the Hawking-Page transition. Note that the flat space limit, which corresponds to keeping g_s small, but fixed and taking the curvature radius of AdS to infinity, is rather subtle. In this limit the stable black hole phase in AdS disappears and the Jeans instability should develop at a certain point. Also note that in the flat space limit, the Hawking-Page temperature goes to zero, which is consistent with the observation that a hot flat spacetime is non-perturbatively unstable at any nonzero temperature [8].

The genus- g contribution F_g to the free energy is obtained by integrating the single string partition function on a genus- g surface over the moduli space \mathcal{M}_g of such surfaces. The potentially divergent contributions to F_g arise from the integration near the boundary of the moduli space.

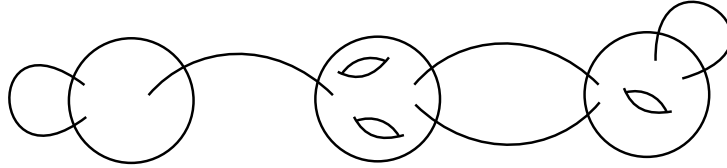


Fig. 1: An example of a degenerate genus-6 Riemann surface. Each blob represents a surface of certain genus and thin lines connecting blobs represent pinched cycles.

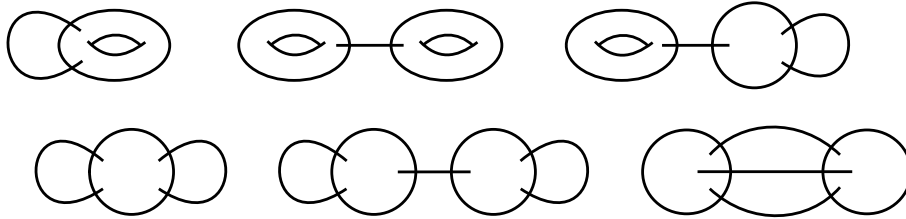


Fig. 2: Degenerate limits of a genus-2 Riemann surface.

The boundary Δ_g of \mathcal{M}_g is where a Riemann surface degenerates, which can be described by pinching cycles on the surface (for reviews see e.g. [16,17,10]). There are two types of basic degenerations depending on whether the pinched cycle is homologous to zero or not. If the pinched cycle is homologous to zero, a surface of genus g degenerates into two surfaces of genus g_1 and g_2 ($g = g_1 + g_2$) which are joined together at a point. If the pinched cycle is not homologous to zero, a genus g surface degenerates into a surface of genus $g - 1$ with two points glued together. One can pinch more than one cycle at the same time as far as they do not intersect with each other. On a genus g surface, the maximal number of nonintersecting closed geodesics is $3g - 3$, so one can pinch at most $3g - 3$ cycles at the same time. See fig. 1 and fig. 2 for examples of degenerate limits.

Let us now examine the contribution to F_g from boundaries of moduli space. The pinching of a Riemann surface can be described in terms of cutting open the path integral on the surface. The pinching is a local operation and so is cutting the path integral

(other than possible constraints from the zero mode integration). We follow the standard procedure as described in [10]. One has

$$\langle 1 \rangle_g = \sum_i q^{h_i} \bar{q}^{\tilde{h}_i} \langle \mathcal{A}_i(z_1) \rangle_{g_1} \langle \mathcal{A}_i(z_2) \rangle_{g_2} \quad (2.5)$$

and

$$\langle 1 \rangle_g = \sum_i q^{h_i} \bar{q}^{\tilde{h}_i} \langle \mathcal{A}_i(z_1) \mathcal{A}_i(z_2) \rangle_{g-1} \quad (2.6)$$

for the two types of basic degenerations, where $\langle \dots \rangle_g$ denote worldsheet correlation functions on a genus g surface and i sums over a complete set of intermediate states. q can be considered as the complex coordinate transverse to the boundary with $q \rightarrow 0$ corresponding to the degeneration limit. Integration of (2.5) and (2.6) near $q \rightarrow 0$ yields the propagator

$$G = \sum_i \frac{8\pi}{\alpha'(-\nabla^2 + m_i^2)}. \quad (2.7)$$

The contribution to the free energy from boundaries of moduli space can be extracted from diagrams like the ones in fig. 1 and fig. 2. One can treat blobs (representing surfaces of certain genus with some insertions) as effective vertices and thin lines (pinched cycles) as propagators. For $\beta \rightarrow \beta_H$ and assuming that the spatial Laplacian operator $-\nabla^2$ has a gap, then the propagator (2.7) for a pinched cycle is potentially dominated by that of the thermal scalar³,

$$G \approx \frac{8\pi}{\alpha' m_\phi^2(\beta)} + \text{finite} \propto \frac{1}{\beta - \beta_H} + \dots, \quad \beta \rightarrow \beta_H \quad (2.8)$$

Since one can pinch at most $3g - 3$ cycles at the same time, naively we may conclude from (2.8) that F_g diverges as $\frac{1}{(\beta - \beta_H)^{3g-3}}$ for $g \geq 2$ as $\beta \rightarrow \beta_H$. However, there are global constraints due to winding number conservation at each blob of fig. 1 and fig. 2. As a result,

³ Note that it is not immediately obvious that the thermal scalar (or other winding modes along the Euclidean time direction) appears in the intermediate states from the point of view of calculating the free energy of a finite temperature string gas, since they do not correspond to spacetime physical states. Indeed in the one-loop calculation, they appear only after a modular transformation. However, it is clear that they should appear in the intermediate states from the point of view that we are working with a string theory compactified on a circle with anti-periodic boundary condition for fermions.

not all propagators can have the nearly-massless thermal scalar propagating through them. We will now show that the most divergent terms at genus g are proportional to

$$\frac{1}{(\beta - \beta_H)^{2g-2}} \quad g \geq 2 . \quad (2.9)$$

Let us consider a generic degenerate limit of a genus g surface as shown for example in fig. 1. Denote $V^{(n,m)}$ the number of vertices with genus n and m insertions. Then the total number L of pinched cycles (propagators) and the genus g of the whole surface can be written as

$$2L = \sum_{n,m} mV^{(n,m)}, \quad g = 1 + \sum_{n,m} \left(\frac{m}{2} + n - 1 \right) V^{(n,m)} . \quad (2.10)$$

The second equation of (2.10) can be obtained from the degenerate rules stated earlier. Alternatively, one can associate each insertion with a factor of g_s and the total power of g_s should be $2(g-1)$. It is also convenient to introduce

$$V = \sum_{n,m} V^{(n,m)}, \quad g_a = \sum_{n,m} nV^{(n,m)}, \quad (2.11)$$

where V is the total number of vertices, g_a is the apparent genus of the diagram (i.e. the sum of the genus of each vertex). Equations (2.10) and (2.11) lead to

$$L - (V - 1) = g - g_a . \quad (2.12)$$

Since winding numbers carried by propagators have to be conserved at each vertex, equation (2.12) implies that the total number of independent windings in a diagram is $g - g_a$. The maximal number of independent windings among different degenerate limits is then g , in which cases each vertex has the topology of a sphere.

From (2.10) and (2.11), we also have

$$V = \frac{1}{2}L - \frac{1}{4} \sum_{n,m} (m-4)V^{(n,m)} \quad (2.13)$$

and (2.13) and (2.12) lead to

$$L = 2(g-1) - \sum_{n,m} \left(2n + \frac{m}{2} - 2 \right) V^{(n,m)} . \quad (2.14)$$

Equation (2.14) implies that the maximal number of propagators (pinched cycles) in a degenerate limit is indeed $3g-3$, obtained when only $V^{(0,3)}$ is nonzero. However, it is impossible to have all $3g-3$ propagators to be divergent at the same time, i.e. to have all windings to be ± 1 , since by winding number conservation if the windings of two of the propagators coming out of a 3-point vertex are ± 1 , then the third one can only be $0, \pm 2$.

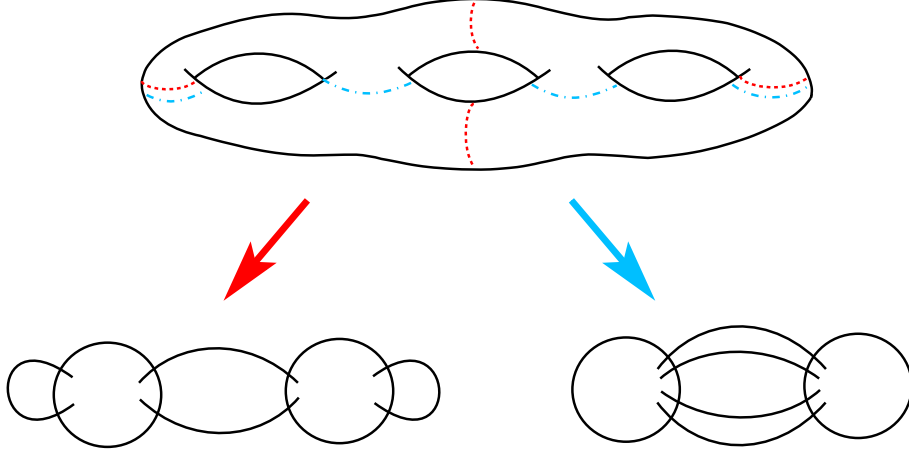


Fig. 3: Two possible degenerate limits of a genus-3 Riemann surface which give rise to most divergent contributions. Each propagator has the thermal scalar running through it.

Since at least one of the propagators going out of a 3-point vertex must have winding $|w| \neq 1$, if our purpose is to find the *maximum* number of propagators that can have $w = \pm 1$, one can ignore such a propagator. This implies we only need to consider those degenerate limits in which effective vertices have at least four insertions, i.e. $m \geq 4$. In the absence of $V^{(0,3)}$, equation (2.14) implies that

$$L \leq 2(g - 1) \quad (2.15)$$

where the equality holds when

$$V^{(0,4)} \neq 0, \quad \text{otherwise } V^{(n,m)} = 0. \quad (2.16)$$

Thus we have proven that the most divergent term is of the form (2.9). See fig. 3 for degenerations which give rise to the most divergent contributions at genus 3.

To summarize, the most divergent contributions at each genus have the following diagrammatic structure:

1. Each vertex has the topology of a sphere and has four winding tachyon operator insertions with winding numbers $1, 1, -1, -1$ respectively. The total number of vertices in a genus g diagram is $g-1$. The path integral over each vertex gives rise to an effective coupling

$$g_s^2 \tilde{\lambda}_4 = \left\langle \mathcal{V}_{+1}(0) \mathcal{V}_{+1}(1) \mathcal{V}_{-1}(\infty) \int d^2 z \mathcal{V}_{-1}(z) \right\rangle_{S^2} \quad (2.17)$$

Note that at $\beta = \beta_H$, the vertex operators $\mathcal{V}_{\pm 1}$ for the thermal scalar are marginal and (2.17) is well defined. Also $\tilde{\lambda}_4$ is g_s -independent.

2. The propagators are given by that of the winding tachyon (2.8). The total number of propagators is $2(g - 1)$.

Thus the most divergent contribution to the free energy at genus- $(n + 1)$ has the form

$$a_n g_s^{2n} \tilde{\lambda}_4^n \left(\frac{8\pi}{\alpha' m_\phi^2(\beta)} \right)^{2n} \propto \frac{g_s^{2n}}{(\beta - \beta_H)^{2n}} \quad (2.18)$$

where a_n is a combinatoric numerical factor depending on the specific geometric structure of boundaries of moduli space. Determining these numerical factors from direct worldsheet computation is a rather complicated mathematical question, which goes beyond the scope of this paper. In the next subsection we will determine them using an indirect argument.

2.3. Double scaling limits and the effective thermal scalar action

In the last subsection we showed that the leading order Hagedorn divergences at all loop orders can be written as

$$F_{sing} = -\log(\beta - \beta_H) + a_1 \frac{\lambda_4 g_s^2}{m_\phi^4} + \dots + a_n \left(\frac{g_s^2 \lambda_4}{m_\phi^4} \right)^n + \dots \quad (2.19)$$

with

$$\lambda_4 = \tilde{\lambda}_4 \left(\frac{8\pi}{\alpha'} \right)^2, \quad m_\phi^2 \approx \frac{\beta_H}{2\pi^2 \alpha'} (\beta - \beta_H). \quad (2.20)$$

Equation (2.19) suggests a double scaling limit

$$\beta - \beta_H \rightarrow 0, \quad g_s \rightarrow 0, \quad \frac{\beta - \beta_H}{g_s} = \text{finite} \quad (2.21)$$

in which case all higher order terms in the series become equally important and we need to be resummed.

How do we interpret the free energy F obtained by resumming the series? A clue comes from the structure of the degenerate diagrams summarized at the end of the last subsection, which resemble the Feynman diagrams of a $|\phi|^4$ theory (see e.g. fig. 3). Indeed the free energy of a $|\phi|^4$ theory gives an asymptotic expansion which is precisely of the form (2.19) with specific values for the numerical coefficients a_n . Given that string theory should reduce to a field theory in the low energy limit, and that here we are essentially isolating

an effective theory for the nearly-massless thermal scalar, it is natural to conjecture that (2.19) can be written as

$$\begin{aligned}
F_{sing} &= \log \int d\phi d\phi^* e^{-m_\phi^2 \phi \phi^* - g_s^2 \lambda_4 (\phi \phi^*)^2} \\
&= -\log(\beta - \beta_H) - 2 \frac{g_s^2 \lambda_4}{m_\phi^4} + 10 \frac{g_s^4 \lambda_4^2}{m_\phi^8} + \dots
\end{aligned}
\tag{2.22}$$

with ϕ is a c-number. Equation (2.22) determines a_n to all orders uniquely and implies the following effective potential for the thermal scalar

$$V = m_\phi^2 \phi \phi^* + \lambda_4 g_s^2 (\phi \phi^*)^2 + \dots .
\tag{2.23}$$

In the next section we will show that the effective action (2.23) and (2.22) arises from the critical behavior of Yang-Mills theories near the Hagedorn temperature. Using AdS/CFT this would serve as a proof of (2.22) for string theories in an asymptotic AdS spacetime. Furthermore, since the factors a_n in (2.18) and (2.19) depend only on the mathematical structure of the moduli space of Riemann surfaces and not on the specific string theory, the Yang-Mills theory results serve as an indirect proof of (2.22).

It is clear from equation (2.22) that Hagedorn divergences at each genus order in (2.19) simply signal breakdown of the asymptotic expansion in g_s due to that ϕ becomes massless. The $m_\phi \rightarrow 0$ limit is apparently smooth in the resummed integral expression (2.22). When λ_4 is positive, i.e. when the transition is second order, the integral (2.22) is finite and non-perturbatively defined. For negative (or zero) λ_4 , i.e. when the transition is first order, the integral (2.22) is not defined non-perturbatively and higher order terms in the effective potential are needed. In either cases the $m_\phi \rightarrow 0$ limit is well-defined.

Equation (2.22) implies that $a_n \sim n!$ for n large. This is in contrast with the $(2n)!$ growth of the asymptotic behavior for the full free energy. Here we are only looking at contributions from boundaries of moduli space, which accounts for the slower growth. When $\lambda_4 < 0$, one can formally resum the series (2.19) or the second line of (2.22) using Borel resummation and one finds that the free energy contains an imaginary part of the form $e^{-\frac{1}{g_s^2}}$ due to the $n!$ growth of a_n . Such an imaginary part can be interpreted as the tunnelling rate from the metastable thermal string gas to the true non-perturbative minimum (see also discussion in [12]).

Here we have been focusing on the lowest spacetime mode⁴ of the thermal scalar, which gives the most divergent contribution to the free energy. This explains the finite-dimensional integral in (2.22). From general covariance it seems natural to generalize (2.23) to include derivatives

$$S = \int d^d x \sqrt{g} (|\partial\phi|^2 + m_\phi^2 \phi\phi^* + \lambda_4 g_s^2 (\phi\phi^*)^2 + \dots) . \quad (2.24)$$

where $d^d x$ integrates over the spatial directions⁵.

Let us now consider the generalization of the above double scaling argument to extract higher orders terms in (2.23). From equation (2.10) the leading contribution of a generic degenerate surface to the free energy can be written in the form

$$\frac{g_s^{2g-2}}{(\beta - \beta_H)^L} = \frac{g_s \sum_{n,k} V^{(n,2k)}(2n+2k-2)}{(\beta - \beta_H) \sum_{n,k} k V^{(n,2k)}} \quad (2.25)$$

where in writing down (2.25) we have assumed that all propagators in a degenerate diagram carry winding numbers⁶ ± 1 and that each vertex contains an even number of insertions $m = 2k, k = 2, 3, \dots$, due to winding number conservation. Now consider the double scaling limit

$$\frac{(\beta - \beta_H)}{g_s^a} = \text{finite}, \quad g_s \rightarrow 0 \quad (2.26)$$

under which (2.25) is proportional to g_s^K with K given by

$$K = \sum_{n=0}^{\infty} \sum_{k=2}^{\infty} V^{(n,2k)}(2n + 2k - 2 - ka) . \quad (2.27)$$

For $a < 1$, we always have $K > 0$ for any choice of $V^{(n,2k)}$. At $a = 1$, we get $K = 0$ for diagrams with $V^{(0,4)} \neq 0$ only while $K > 0$ for all other diagrams. In the double scaling limit (2.26) only the contributions of diagrams with $K = 0$ survive. These are the most

⁴ Recall that we assume that the Laplacian of the spacetime manifold has a mass gap.

⁵ Note that for an AdS with a small negative cosmological constant, (2.24) applies to regions in the interior of the spacetime, since in AdS g_{tt} component of the metric is nontrivial and the thermal scalar always has a large mass near the boundary.

⁶ If there is a propagator carrying a winding number other than ± 1 , we can treat the two vertices connected by this propagator as a single effective vertex. Keeping doing this we obtain a degenerate diagram whose propagators only carry winding numbers ± 1 .

divergent contributions we isolated in (2.19) and lead to the effective action (2.23). Now let us set by hand $\lambda_4 = 0$, then in (2.27), $V^{(0,4)} = 0$. The most divergent contributions in the remaining diagrams are isolated by taking $a = \frac{4}{3}$, at which $K = 0$ for diagrams with $V^{0,6} \neq 0$ only and $K > 0$ for all the rest. In other words now the most divergent contributions to the free energy can be written as

$$F = -\log(\beta - \beta_H) + \frac{c_1 g_s^2}{(\beta - \beta_H)^{\frac{3}{2}}} + \dots + \frac{c_n g_s^{2n}}{(\beta - \beta_H)^{\frac{3n}{2}}} + \dots \quad (2.28)$$

which implies the effective potential

$$V = m_\phi^2 \phi \phi^* + \lambda_6 (\phi \phi^*)^3 + \dots \quad (2.29)$$

where λ_6 is related to the genus-0 six-point function of the vertex operators for the thermal scalar on the worldsheet. Now restoring λ_4 and combining (2.22) and (2.29) we would conclude that the effective potential can be written as

$$V = m_\phi^2 \phi \phi^* + \lambda_4 (\phi \phi^*)^2 + \lambda_6 (\phi \phi^*)^3 + \dots \quad (2.30)$$

The same procedure can then be repeated to the next order by first setting λ_4 and λ_6 to zero and then extracting the most divergent terms in the remaining diagrams. One can continue this to arbitrary orders in $(\phi \phi^*)^n$ and we find the effective potential⁷

$$V = m_\phi^2 \phi \phi^* + \sum_{k=2}^{\infty} \lambda_{2k} g_s^{2k-2} (\phi \phi^*)^k + \dots \quad (2.31)$$

The λ_{2k} term is obtained by setting all vertices with $m < 2k$ to zero and performing the scaling $\beta - \beta_H \sim g_s^{2(1-\frac{1}{k})}$, i.e. $a = 2(1 - \frac{1}{k})$ in (2.26).

Finally let us consider how to define various $\lambda_6, \lambda_8, \dots$ from string amplitudes. Recall that λ_4 can be obtained from (2.17) and (2.20). Naively one might want to define λ_{2k} for $k = 3, 4, \dots$ by the *tree-level* amplitudes of k winding 1 and k winding -1 modes. However, from factorization argument, these amplitudes are divergent at $m_\phi^2 = 0$. The divergences come from diagrams containing lower order vertices $\lambda_{2k'}$ with $k' < k$ and ϕ in the internal propagators, which can be found from standard Feynman diagrams for the action $m_\phi^2 \phi \phi^* + \sum_{k'=2}^{k-1} \lambda_{2k'} g_s^{2k'-2} (\phi \phi^*)^{k'}$. λ_{2k} is thus given by the sphere amplitude of k winding 1 and k winding -1 modes with the divergent parts subtracted.

⁷ Note that the procedure is not well adapted to resum divergences due to vertices with genus $n \geq 1$. From (2.27), to have $K = 0$ for $n = 1$, we need $a = 2$, in which case all genus 1 vertices with arbitrary number of insertions contribute equally. To have $K = 0$ for $n > 1$, we need $a > 2$, then from (2.27), diagrams with large k become more dominant regardless of the value of n .

3. Hagedorn behavior from YM theories

Our discussion in the last section was rather generic. In particular it should apply to type IIB string theory in $AdS_5 \times S_5$ or other string theories in asymptotic AdS spacetime. In an AdS spacetime with curvature radius R much bigger than the string and Planck lengths, there is a first order Hawking-Page transition at temperature $T_{HP} \sim \frac{1}{R}$ much below the Hagedorn temperature $T_H \sim \frac{1}{\sqrt{\alpha'}}$ at which the thermal string gas in AdS becomes perturbatively unstable [15]. The discussion of the last section describes what happens if one stays in the superheated thermal AdS phase above the Hawking-Page temperature all the way to the Hagedorn temperature. From the critical behavior at the Hagedorn temperature one can then map out the potential for the thermal scalar. Aspects of the Hagedorn transition in AdS have been discussed in [18,14].

Hawking and Page's semi-classical discussion applies to IIB string theory in AdS with a cosmological constant small compared to the string scale and to the Planck scale, which corresponds to $\mathcal{N} = 4$ super-Yang-Mills theory on S^3 at strong 't Hooft coupling [19]. At zero and weak 't Hooft coupling, which is dual to a small AdS, thermodynamics of $\mathcal{N} = 4$ SYM theory on S^3 has been discussed in [20,21]. In the free theory limit the Hagedorn and Hawking-Page temperatures coincide. At weak coupling it is not yet clear whether the transition is of first or second order [21]. Other studies of (Hagedorn) phase transitions in Yang-Mills theories include [11,12,22-35].

In this section we show that the critical Hagedorn behavior found in the last section arises also for a wide class of matrix quantum mechanical systems including $\mathcal{N} = 4$ SYM on S^3 . Our discussion applies regardless of the order of the transition and also to strong coupling. In particular, we show explicitly that the Hagedorn divergences can be attributed to an effective potential of the form (2.31), which was only argued in the last section.

The plan of this section is as follows. In next subsection we introduce the family of theories to which our discussion applies, which includes $\mathcal{N} = 4$ SYM on S^3 . In the subsequent subsections we discuss the large N expansion of these theories at finite temperature and identify new ingredients. We show that the free energy contain contributions from “vortices” and introduce a set of vortex diagrams to describe them. The vortex diagrams can be identified with degenerate worldsheets on the string theory side. The critical behavior near the Hagedorn temperature and the effective action for the thermal scalar are recovered at the end.

3.1. Theories of interest

Consider the following class of matrix quantum mechanical systems

$$S = \int_0^\beta d\tau \left[N \text{tr} \sum_\alpha \left(\frac{1}{2} (D_\tau M_\alpha)^2 - \frac{1}{2} \omega_\alpha^2 M_\alpha^2 \right) + N \text{tr} \sum_a \xi_a^\dagger (D_\tau + \tilde{\omega}_a) \xi_a + V(M_\alpha, \xi_a; \lambda) \right] \quad (3.1)$$

where:

1. We have written the action in Euclidean signature, with the Euclidean time τ having a period $\beta = \frac{1}{T}$. In the zero temperature limit, $\beta \rightarrow \infty$.
2. M_α and ξ_a are $N \times N$ bosonic and fermionic matrices respectively, and

$$D_\tau M_\alpha = \partial_\tau M_\alpha - i[A, M_\alpha], \quad D_\tau \xi_a = \partial_\tau \xi_a - i[A, \xi_a] . \quad (3.2)$$

are covariant derivatives. As a result, (3.1) has a $U(N)$ gauge symmetry, with M_α, ξ_a transforming in the adjoint representation. The (0+1)-dimensional ‘‘gauge field’’ $A(\tau)$ plays the role of the Lagrange multiplier which imposes that physical states are singlet of $U(N)$. M_α, ξ_a satisfy periodic and anti-periodic boundary conditions respectively

$$M_\alpha(\tau + \beta) = M_\alpha(\tau), \quad \xi_a(\tau + \beta) = -\xi_a(\tau) . \quad (3.3)$$

3. The frequencies ω_α and $\tilde{\omega}_a$ in (3.1) are nonzero for any α and a , i.e. the theory has a mass gap and a unique vacuum. The number of matrices is greater than one and can be infinite.
4. $V(M_\alpha, \xi_a; \lambda)$ can be written as a sum of *single-trace* operators and is controlled by a coupling constant λ , which remains fixed in the large N limit.

$\mathcal{N} = 4$ SYM on S^3 is an example of such systems with an infinite number of matrices when the Yang-Mills and matter fields are expanded in terms of spherical harmonics on S^3 . $V(M_\alpha, \xi_a; \lambda)$ can be schematically written as⁸

$$V = N \left(\sqrt{\lambda} V_3(M_\alpha, \xi_a) + \lambda V_4(M_\alpha, \xi_a) \right) \quad (3.4)$$

⁸ The precise form of the interactions depends on the choice of gauge. It is convenient to choose Coulomb gauge $\nabla \cdot \vec{A} = 0$, in which the longitudinal component of the gauge field is set to zero. In this gauge, M_α include also non-propagating modes coming from harmonic modes of ghosts and the zero component of the gauge field.

where V_3 and V_4 contain infinite sums of single-trace operators which are cubic and quartic in M_α, ξ_a . $\lambda = g_{YM}^2 N$ is the 't Hooft coupling.

To end this subsection, let us recall the standard relation between the large N expansion of a matrix quantum mechanics like (3.1) (or a gauge field theory) *at zero temperature* with the string theory perturbative expansion [36]. In the large N limit, the free energy of (3.1) can be organized in terms of the topology of Feynman diagrams

$$\log Z = \sum_{h=0}^{\infty} N^{2(1-h)} f_h(\lambda) \quad (3.5)$$

where $f_0(\lambda)$ is the sum of connected planar Feynman diagrams, and $f_1(\lambda)$ is the sum of connected non-planar diagrams which can be put on a torus, and so on. The expansion (3.5) resembles the perturbative expansion of a string theory, with $1/N$ identified with the closed string coupling g_s and $f_h(\lambda)$ identified with contributions from worldsheets of genus- h . For $\mathcal{N} = 4$ SYM theory on S^3 , $f_h(\lambda)$ is the contribution of string worldsheets of h handles propagating in $AdS_5 \times S_5$.

In the next few subsections, we discuss the large N expansion of (3.1) at finite temperature, and new ingredients arise. We find new contributions associated with Feynman diagrams with vortices, which can be identified with degenerate limits of a string worldsheet. As a result, the same critical Hagedorn behavior is recovered from gauge theories.

3.2. Correlation functions in free theory

In this subsection we discuss finite temperature correlation functions of (3.1) in the free theory limit (i.e. with $V = 0$), focusing on the large N counting. We will find that at finite temperature, in addition to the standard $1/N^2$ corrections due to non-planar diagrams, there are corrections due to vortices. This subsection makes preparation for the discussion of the interacting theory free energy in the next subsection.

(3.1) has a $U(N)$ gauge symmetry, which can be used to set the gauge field $A(\tau)$ to zero. The gauge transformation, however, modifies the boundary conditions from (3.3) to

$$M_\alpha(\tau + \beta) = U M_\alpha U^\dagger, \quad \xi_a(\tau + \beta) = -U \xi_a U^\dagger. \quad (3.6)$$

The unitary matrix U can be understood as the Wilson line of A wound around the τ direction (Polyakov loop), which cannot be gauged away. Correlation functions can then be written in terms of a path integral as

$$\langle \dots \rangle_{0,\beta} = \frac{1}{Z_0(\beta)} \int dU \int DM_\alpha(\tau) D\xi_a(\tau) \dots e^{-S_0[M_\alpha, \xi_a; A=0]} \quad (3.7)$$

with M_α, ξ_a satisfying the boundary conditions (3.6). S_0 and Z_0 are the action and partition function for the free theory respectively. The free theory action S_0 has only quadratic dependence on M_α and ξ_a , thus the functional integrals over these variables in (3.7) can be carried out explicitly and (3.7) can be reduced to a matrix integral over U only.

The free theory partition function can be written as [20,21]

$$Z_0(\beta) = \int dU e^{I_0(U)} \quad (3.8)$$

with $I_0(U)$ given by

$$I_0(U) = \sum_{n=1}^{\infty} \frac{1}{n} V_n(\beta) \text{Tr} U^n \text{Tr} U^{-n} \quad (3.9)$$

and

$$V_n(\beta) = z_b(n\beta) + (-1)^{n+1} z_f(n\beta), \quad z_b(\beta) = \sum_{\alpha} e^{-\beta\omega_{\alpha}}, \quad z_f(\beta) = \sum_a e^{-\beta\tilde{\omega}_a}. \quad (3.10)$$

When the temperature T is small, the matrix integral (3.8) can be evaluated in the large N limit as [20,21]

$$Z_0(\beta) = C \prod_{n=1}^{\infty} \frac{n}{1 - V_n(\beta)} + O(1/N^2) \quad (3.11)$$

where C is an N -independent constant factor. $Z_0(\beta)$ becomes divergent if some $V_n(\beta)$ are equal to 1. From (3.10) one can check that $V_1(\beta) > V_n(\beta)$ for $n > 1$ and that $V_1(\beta)$ is a monotonically increasing function of T , with $V_1(\beta = \infty) = 0$ and $V_1(\beta = 0) > 1$. Thus as one increases T from zero, there exists a T_H , at which $V_1(T_H) = 1$ and Z_0 becomes divergent. Equation (3.11) only applies to $T < T_H$. As pointed out in [20,21], the divergence is precisely of the Hagedorn-type (2.4) for a string theory in a spacetime whose Laplacian has a gap. The critical behavior of higher order terms in (3.11) near T_H and the smoothing of the Hagedorn divergence at finite N (i.e. in quantum string theory) for free Yang-Mills theory was further discussed in [11].

Correlation functions of gauge invariant operators can be obtained by first performing Wick contractions and then evaluating the matrix integral for U . With boundary conditions (3.6), the contractions of M_a and ξ_a are [37]

$$\underbrace{M_{ij}^a(\tau) M_{kl}^b(0)} = \frac{\delta_{ab}}{N} \sum_{m=-\infty}^{\infty} G_s(\tau - m\beta; \omega_a) U_{il}^{-m} U_{kj}^m \quad (3.12)$$

$$\underbrace{\xi_{ij}^a(\tau) \xi_{kl}^b(0)} = \frac{\delta_{ab}}{N} \sum_{m=-\infty}^{\infty} (-1)^m G_f(\tau - m\beta; \tilde{\omega}_a) U_{il}^{-m} U_{kj}^m$$

where G_s and G_f are standard $(0+1)$ -dimensional propagators at zero temperature

$$G_s(\tau; \omega) = \frac{1}{2\omega} e^{-\omega|\tau|}, \quad G_f(\tau; \omega) = (-\partial_{\tau} + \omega) G_s(\tau; \omega). \quad (3.13)$$

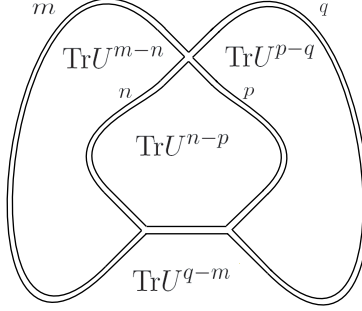


Fig. 4: An example of a double-line diagram at finite temperature. Each propagator carries a winding number (or image number), which should be summed over. Due to the presence of U -factors in (3.12), associated with each face one finds a factor of $\text{tr}U^{s_A}$, instead of a factor N as is the case at zero temperature.

It follows from (3.12) that at finite temperature, each propagator in a double-line Feynman diagram carries a winding number (or image number) m , which should be summed over (see fig. 4). More explicitly, using (3.12), the contribution of a generic Feynman diagram to a correlation function of single-trace operators⁹ can be written in the form¹⁰ [37]

$$\frac{1}{N^{2h-2}} \left(\prod_{i \leq j} \prod_{p=1}^{I_{ij}} \sum_{m_{ij}^{(p)} = -\infty}^{\infty} \right) \left(\prod_{i \leq j} \prod_{p=1}^{I_{ij}} G_s^{(p)}(\tau_{ij} - m_{ij}^{(p)} \beta) \right) \left\langle \frac{1}{N} \text{tr}U^{s_1} \frac{1}{N} \text{tr}U^{s_2} \dots \frac{1}{N} \text{tr}U^{s_F} \right\rangle_U \quad (3.14)$$

where i, j enumerate the vertices (i.e. operator insertions) and p enumerates the propagators between vertices i and j with I_{ij} the total number of propagators between them. $m_{ij}^{(p)}$ label the images of $G^{(p)}(\tau_{ij})$. h is the genus of the diagram. In (3.14),

$$\langle \dots \rangle_U = \frac{1}{Z_0(\beta)} \int dU \dots e^{I_0(U)} \quad (3.15)$$

with $I_0(U)$ given by (3.9). The powers s_1, s_2, \dots in the last factor of (3.14) can be found as follows. To each propagator in the diagram we assign a direction and an orientation can be chosen for each face. For each face A in the diagram, we have a factor $\text{tr}U^{s_A}$, with s_A given by

$$s_A = \sum_{\partial A} (\pm) m_{ij}^{(p)}, \quad A = 1, 2, \dots, F \quad (3.16)$$

⁹ We assume the operators are normalized as $N \text{tr}(\dots)$.

¹⁰ For notational simplicity, we only include bosonic modes in the equation below. It can be easily generalized to include fermions.

where the sum ∂A is over the propagators bounding the face A and F denotes the total number of faces in a diagram (see e.g. fig. 4). In (3.16) the plus (minus) sign is taken if the direction of the corresponding propagator is the same as (opposite to) that of the face. s_A has a precise mathematical meaning: it is the number of times that the Euclidean time circle is wrapped around by the propagators bounding a face A . We will thus call s_A the vortex number for face A . Note that since the exponents of U add up to zero in (3.12), for each *connected part* of a Feynman diagram the sum of s_A adds to zero. To illustrate more explicitly how (3.14) works, we give some examples in Appendix A.

The partition function (3.8) and more generally matrix integrals in (3.14) can be evaluated to all orders in a $1/N^2$ expansion. In Appendix B we prove that, *up to corrections non-perturbative in N* , the matrix integrals can be evaluated by treating each $\text{Tr}U^n$ as an independent integration variable. More explicitly, (3.15) can be evaluated by replacing

$$\frac{1}{N}\text{Tr}U^n \rightarrow \phi_n, \quad \frac{1}{N}\text{Tr}U^{-n} \rightarrow \phi_{-n} = \phi_n^*, \quad \phi_0 = 1, \quad (3.17)$$

i.e.

$$\begin{aligned} & \left\langle \frac{1}{N}\text{Tr}U^{s_1} \frac{1}{N}\text{Tr}U^{s_2} \dots \frac{1}{N}\text{Tr}U^{s_F} \right\rangle_U \\ &= \frac{1}{Z_0} \int_{-\infty}^{\infty} \left(\prod_{i=1}^{\infty} d\phi_i d\phi_i^* \right) \phi_{s_1} \dots \phi_{s_F} \exp \left(-N^2 \sum_{n=1}^{\infty} v_n(\beta) \phi_n \phi_n^* \right) \\ & \quad + \text{nonperturbative in } N \end{aligned} \quad (3.18)$$

where

$$v_n(\beta) = \frac{1 - V_n(\beta)}{n}. \quad (3.19)$$

From (3.18),

$$\begin{aligned} & \left\langle \frac{1}{N}\text{Tr}U^{s_1} \frac{1}{N}\text{Tr}U^{s_2} \dots \frac{1}{N}\text{Tr}U^{s_F} \right\rangle_U \\ &= \prod_{i=1}^F \delta_{s_i,0} + \frac{1}{N^2} \sum_{i < j=1}^F \left(\frac{1}{v_{|s_i|}(\beta)} \delta_{s_i+s_j,0} \prod_{k=1}^F \delta_{s_k,0} \right) \\ & \quad + O(N^{-4}) + \text{nonperturbative in } N \end{aligned} \quad (3.20)$$

where order $1/N^2$ terms are obtained by contractions of one pair of ϕ_{s_i} 's, order $1/N^4$ terms are obtained by contracting two pairs of ϕ 's, and so forth. Each contraction brings a factor of $\frac{1}{N^2 v_{s_i}(\beta)}$. Perturbative corrections in $1/N^2$ terminate at order $1/N^F$ (or $1/N^{F-1}$)

for F even (odd). For example, there is no other perturbative correction in $1/N^2$ for the partition function (3.11), and for $F = 2$

$$\left\langle \frac{1}{N} \text{tr} U^n \frac{1}{N} \text{tr} U^m \right\rangle = \delta_{n,0} \delta_{m,0} + \frac{1}{N^2} \frac{1}{v_{|n|}(\beta)} \delta_{m+n,0} + \text{nonperturbative corrections} . \quad (3.21)$$

To summarize, combining (3.14) and (3.20) we find that for a correlation function of gauge invariant operators, there are two sources of $1/N^2$ corrections:

1. From the genus of the diagram as indicated by the power of $1/N$ in (3.14). This follows from the standard large N counting.
2. From the $1/N^2$ corrections of the matrix integral (3.20). The leading order term in (3.20) imposes the constraint that for any face A of the diagram the vortex number s_A should be zero. The next order corresponds to having nonzero vortex numbers in two of the faces, say the faces A and B with $s_A s_B \neq 0$ and $s_A + s_B = 0$. Below, we will refer to those diagrams with nonzero vortex numbers as containing vortices, in anticipation of their interpretation from the string worldsheet¹¹. From remarks below (3.16), if a face A of a Feynman diagram contains a vortex with vortex number s_A , then the propagators bounding the face wrap around the Euclidean time circle s_A times. At finite temperature, due to the presence of vortices, planar diagrams also contain higher order $1/N^2$ corrections.

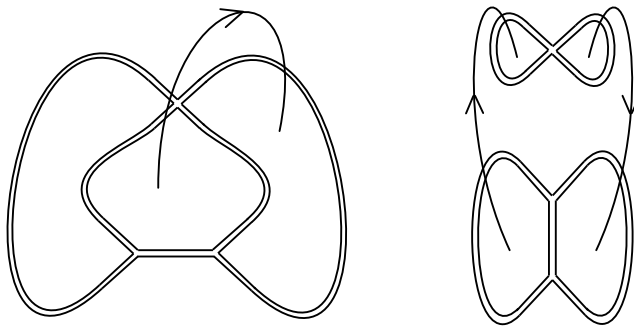


Fig. 5: Examples of double-line diagrams with nonzero vortices. Each thin line (vortex propagator) represents a contraction in (3.20). Compare the left diagram to fig. 4. Diagrams which are disconnected at zero temperature can be connected through vortex propagators as in the right diagram.

¹¹ See also the discussion of [38] in the context of $c = 1$ matrix models.

It will be convenient to represent the vortex contributions diagrammatically: we represent each contraction in (3.20) by an oriented line between two surfaces which have the opposite vortex numbers. The orientation of a line is that it exists (enters) the surface if its vortex number is positive (negative). We associate a factor $1/N$ for each vortex and a factor $1/v_n(\beta)$ to a line (vortex propagator) connecting two surfaces with vortex number $\pm n$. See fig. 5 for some examples of such diagrams. Note that a diagram with otherwise disconnected parts connected by vortex lines should be considered as connected, as in the right diagram of fig. 5. In computing a correlation function one should sum over all possible vortex contributions.

To summarize this subsection, in computing correlation functions at finite temperature, one should consider not only Feynman diagrams which appear at zero temperature, but also diagrams with nonzero vortices. Explicit examples are given in Appendix A.

3.3. Free energy in interacting theory and vortex diagrams

We now consider the Euclidean partition function of the interacting theory. Our purpose is to identify T_H and the critical behavior near T_H to all orders in the $1/N^2$ expansion.

In perturbation theory, the partition function can be evaluated by expanding the interaction terms in the exponent of the path integral

$$Z(\beta, \lambda) = Z_0(\beta) \sum_{n=0}^{\infty} \frac{(-1)^n}{n!} \int_0^\beta \prod_{i=1}^n d\tau_i \langle V(\tau_1) \cdots V(\tau_n) \rangle_{0,\beta} \quad (3.22)$$

In (3.22), $\langle \cdots \rangle_{0,\beta}$ denotes free theory correlation functions and recall that V is given by a sum of single trace operators of the form $N \text{tr}(\cdots)$. The free energy can be obtained from

$$\log Z = \log Z_0 + \sum_{n=0}^{\infty} \frac{(-1)^n}{n!} \int_0^\beta \prod_{i=1}^n d\tau_i \langle V(\tau_1) \cdots V(\tau_n) \rangle_{0,\beta, \text{connected}} \quad (3.23)$$

i.e. one sums only over the connected diagrams. The discussion in the last subsection for free theory correlation functions can now be directly carried over to $\log Z$. In particular, there are two sources of $1/N^2$ corrections: from the non-planar structure and from vortices. We can expand $\log Z$ in $1/N^2$ as

$$\log Z(\beta) = \sum_{n=0}^{\infty} N^{2-2n} \mathcal{Z}_n(\beta) = N^2 \mathcal{Z}_0(\beta) + \mathcal{Z}_1(\beta) + \frac{1}{N^2} \mathcal{Z}_2(\beta) + \cdots \quad (3.24)$$

where \mathcal{Z}_0 corresponds to the sum over connected planar diagrams with no vortices, while \mathcal{Z}_1 contains the sum of connected genus-1 non-planar diagrams with no vortices *and* planar diagrams with one pair of vortices, and so on. Recall that each vortex carries a factor $1/N$ and they always come in pairs. Also as remarked at the end of the last subsection, a diagram with otherwise disconnected parts connected by vortex propagators is connected.

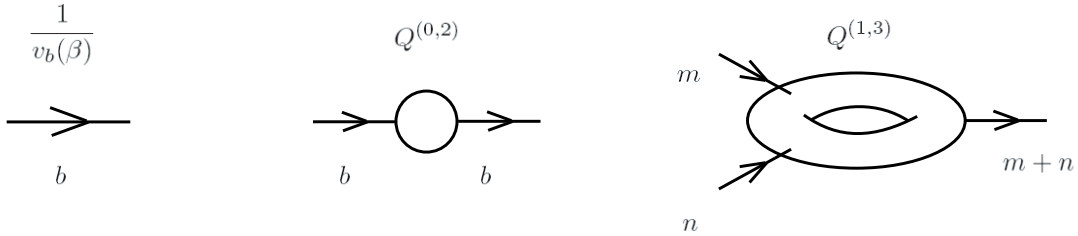


Fig. 6: The propagators and vertices for vortex diagrams. The vertices $Q^{(h,n)}$ of a vortex diagram have n legs, each of which is labelled by a vortex number. The sign of the vortex number is positive (negative) if the corresponding leg exists (enters) the vertex. The total vortex number of a vertex is zero. We show $Q^{(0,2)}$, $Q^{(1,3)}$ in the figure as illustrations.

To elucidate the structure of \mathcal{Z}_g , we introduce a new set of “vortex diagrams”, by generalizing the diagrammatical rules introduced below fig. 5:

1. Denote $Q^{(h,n)}$ as the sum of connected Feynman diagrams with genus h and with n vortices. In terms of large N counting, $Q^{(h,n)}$ is of order N^{2-2h-n} , as we associate a factor $1/N$ with each vortex. Each vortex is labeled by a vortex number and the total vortex number carried by $Q^{(h,n)}$ is zero¹². Diagrammatically, $Q^{(h,n)}$ are represented as vertices with n oriented legs. The leg exits the vertex if the corresponding vortex number is positive.
2. Vortex diagrams are then constructed following the usual rules with $Q^{(h,n)}$ as fundamental vertices and $1/v_b(\beta), b > 0$ as propagators. Note that b is the vortex number carried by a propagator and v_b was defined in (3.19).
3. The combinatoric rules are the same as standard Feynman diagram. In particular, if there are m identical vertices $Q^{(h,n)}$ in a diagram, there is a factor $1/m!$, which comes from the fact that disconnected diagrams are obtained from connected ones by exponentiation.

¹² This follows from the discussion below (3.16).

Using the above diagrammatical rules, we now enumerate the contributions to \mathcal{Z}_g . See fig. 6 for illustrations of propagators and vertices for vortex diagrams.

Let us first look at \mathcal{Z}_0 , which is given by the sum of all planar diagrams without vortex. In section 4 of [37] it was shown that \mathcal{Z}_0 is identical to the corresponding expression at zero temperature and thus is temperature-independent¹³. Since the free energy $-\beta F$ is defined by subtracting the zero-temperature contribution (which is the vacuum energy) from (3.24), we conclude that the planar contribution to the free energy is identically zero¹⁴.

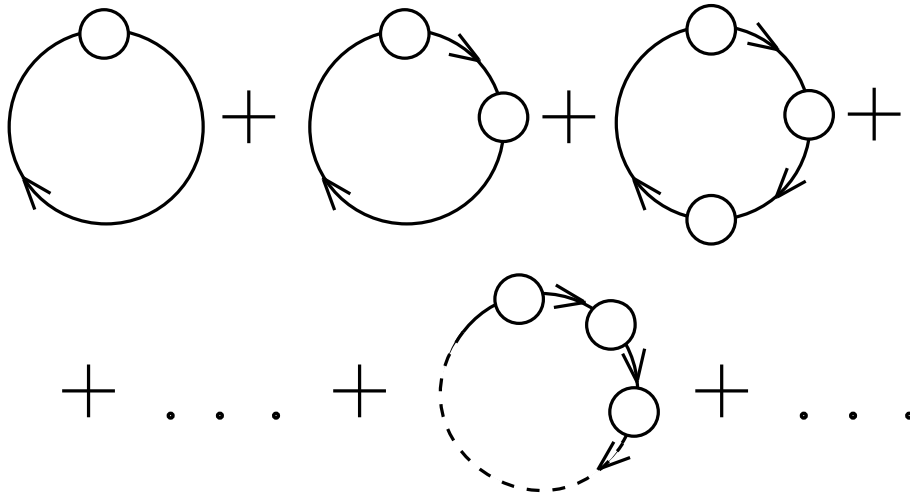


Fig. 7: Vortex diagrams contributing to $\mathcal{Z}_1^{(3)}$.

We now look at \mathcal{Z}_1 , which contains three contributions: (i) genus-1 contribution in free theory coming from the first term in (3.23); (ii) sum of genus-1 Feynman diagrams with no vortices; (iii) planar diagrams with vortices. The first contribution $\mathcal{Z}_1^{(1)}$ is given by the logarithm of (3.11). The second contribution $\mathcal{Z}_1^{(2)}$ is given by $Q^{(1,0)}$. To find the third contribution $\mathcal{Z}_1^{(3)}$, let us denote $Q_b^{(0,2)}$ the sum of all planar connected diagrams with two vortices of winding $\pm b$. Graphically, it can be represented by a sphere with an arrow pointing in and an arrow pointing out, each carrying vortex number b , as in the second diagram of fig. 6. Using $Q_b^{(0,2)}$, $\mathcal{Z}_1^{(3)}$ is obtained by summing the vortex diagrams in fig. 7.

¹³ \mathcal{Z}_0 is a special case of the discussion in section 4 of [37] with no external operator insertions.

¹⁴ as is the case for a string theory below the Hagedorn temperature.

The combinatoric factor for a diagram with m vertices is $1/m$ following from the cyclic symmetry and we find that

$$\mathcal{Z}_1^{(3)} = \sum_{b=1}^{\infty} \sum_{m=1}^{\infty} \frac{1}{m} \left(\frac{Q_b^{(0,2)}(\lambda, \beta)}{v_b(\beta)} \right)^m = - \sum_{b=1}^{\infty} \log \left(1 - \frac{Q_b^{(0,2)}(\lambda, \beta)}{v_b(\beta)} \right). \quad (3.25)$$

Adding all three contributions together we find that

$$\begin{aligned} \mathcal{Z}_1 &= \mathcal{Z}_1^{(1)} + \mathcal{Z}_1^{(2)} + \mathcal{Z}_1^{(3)} \\ &= Q^{1,0}(\beta, \lambda) - \sum_{b=1}^{\infty} \left(\log \left(1 - \frac{Q_b^{(0,2)}(\lambda, \beta)}{v_b(\beta)} \right) + \log v_b(\beta) \right) \\ &= Q^{1,0}(\beta, \lambda) - \sum_{b=1}^{\infty} \log \left(v_b(\beta) - Q_b^{(0,2)}(\lambda, \beta) \right). \end{aligned} \quad (3.26)$$

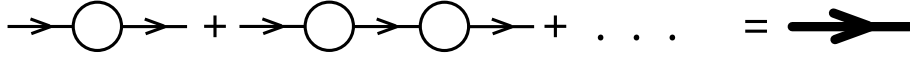


Fig. 8: The dark thick line represents the resummed propagator $\mathcal{G}_b = \frac{1}{v_b - Q_b^{(0,2)}}$.

It should be clear from the above discussion of $\mathcal{Z}_1^{(3)}$ that $Q_b^{(0,2)}$ should not really be treated as a vertex. Rather all $Q_b^{(0,2)}$ should be resummed along with the propagators $\frac{1}{v_b(\beta)}$ to obtain a "resummed propagator" for each vortex number

$$\mathcal{G}_b(\beta) = \sum_{n=1}^{\infty} \frac{1}{v_b^n(\beta)} (Q_b^{(0,2)})^n = \frac{1}{v_b - Q_b^{(0,2)}} \quad (3.27)$$

as shown diagrammatically in fig. 8. Note that (3.26) can be rewritten in terms of \mathcal{G}_b as

$$\mathcal{Z}_1 = Q^{1,0}(\beta, \lambda) + \sum_{b=1}^{\infty} \log \mathcal{G}_b(\beta). \quad (3.28)$$

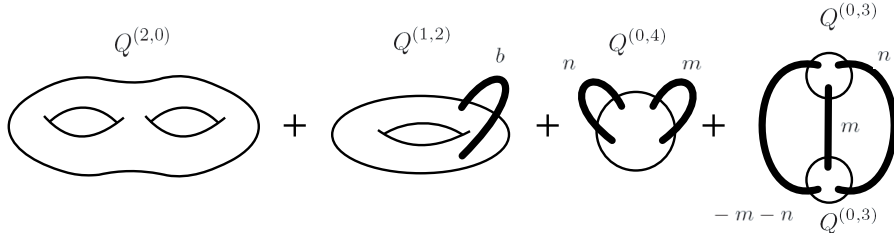


Fig. 9: Vortex diagrams contributing to \mathcal{Z}_2 . Compare plots in fig. 9 with the degenerate limits of a genus-2 surface in fig. 2. Note the 2nd, 3rd and 5th diagrams in fig. 2 do not appear in the above since they contain propagators which have to have zero windings.

In the vortex diagrams for \mathcal{Z}_g with $g \geq 2$, only resummed propagators \mathcal{G}_b appear. As an example, the vortex diagrams contributing to \mathcal{Z}_2 are shown in fig. 9. Higher order diagrams contributing to general \mathcal{Z}_g can be similarly constructed.

By now readers may have recognized the resemblance of vortex diagrams with the diagrams in fig. 1 and fig. 2. Indeed it is natural to identify vortex diagram contributions in the gauge theory with contributions from degenerate limits of string worldsheets in the corresponding string theory. For example, diagrams in fig. 9 can be identified with various degenerate limits (fig. 2) of genus two Riemann surfaces. In particular, vortices in gauge theory vortex diagrams can be identified with insertions of winding tachyon modes in the worldsheet. On the worldsheet if one follows a closed contour around the vertex operator of a winding tachyon mode of winding number b , the Euclidean time circle is traversed b times. Similarly, as discussed earlier if a face of a Feynman diagram contains a vortex with vortex number b , the propagators bounding the face wrap around the Euclidean time circle b times.

A more careful comparison between vortex diagrams for \mathcal{Z}_g and degenerate limits of a genus- g surface (e.g. between fig. 9 and fig. 2) also show some important differences:

1. Notice that the 2nd, 3rd and 5th diagrams in fig. 2 do not appear in fig. 9. These diagrams are distinguished in that some propagators are forced to have zero winding due to winding number conservation. One can convince oneself that this feature persists to all orders. Thus YM vortex diagrams do not correspond to the full contributions from degenerate limits of a Riemann surface. All propagators in the YM vortex diagrams carry nonzero windings.
2. Various degenerate limits of a Riemann surface do not follow the standard Feynman rules and cannot be treated as Feynman diagrams. For example, the third diagram of fig. 2 can be obtained as a degenerate limit of the first diagram and the fifth as a limit of the fourth, etc. In contrast, the vortex diagrams we constructed in Yang-Mills theory do follow standard Feynman rules. In particular, different diagrams in fig. 9 do not overlap.

Thus vortex diagrams correspond to a specific decomposition of the boundary of the moduli space and can be considered as defining an effective string field theory for the winding tachyon modes.

3.4. Critical Hagedorn behavior and the effective action

Now let us examine the critical Hagedorn behavior of (3.24) by increasing the temperature from zero.

In free theory, as reviewed after equation (3.11), there is a Hagedorn temperature given by equation $V_1(\beta_H) = 1$ at which the free energy diverges as $\log Z_0 \approx -\log(\beta - \beta_H)$. Note that there is *only* a one-loop divergence since all perturbative corrections in $1/N$ to (3.11) vanish.

In the interacting theory the effective vertices $Q^{(h,n)}$ should be regular at any temperature since they involve only sums of products of (3.13) and their images. The divergences of \mathcal{Z}_n then can only occur when the resummed propagator $\mathcal{G}_b(\beta)$ (3.27) become divergent, which happens when

$$v_b(\beta) = Q_b^{(0,2)}(\lambda, \beta), \quad \text{i.e.} \quad \frac{1 - V_b(\beta)}{b} = Q_b^{(0,2)}(\lambda, \beta), \quad b = 1, 2, \dots \quad (3.29)$$

If we again assume that (3.29) is first satisfied for $b = 1$ as one decreases β from infinity¹⁵, the Hagedorn temperature in the interacting theory is determined by

$$V_1(\beta_H(\lambda)) = 1 - Q_1^{(0,2)}(\lambda, \beta_H(\lambda)) \quad (3.30)$$

with the most divergent term in \mathcal{Z}_1 given by (see (3.26))

$$\mathcal{Z}_1 \approx -\log(\beta - \beta_H(\lambda)) + \text{finite}, \quad \beta \sim \beta_H(\lambda) . \quad (3.31)$$

Divergences in \mathcal{Z}_n can be analyzed following exactly the same power counting argument of the last section (after equation (2.9)). We find that the most divergent contribution to \mathcal{Z}_n as $\beta \rightarrow \beta_H$ is given by

$$\frac{1}{(\beta - \beta_H)^{2n}} . \quad (3.32)$$

Furthermore, since the construction of vortex diagrams follows the standard combinatoric rules of Feynman diagrams, we find that the most divergent pieces at each $1/N^{2h}$ order is precisely given by (2.22) with the identification

$$m_\phi^2 = v_1(\beta) - Q_1^{(0,2)}(\lambda, \beta), \quad \frac{\lambda_4}{N^2} = Q_{1,1,-1,-1}^{(0,4)} + \frac{1}{v_2(\beta) - Q_2^{(0,2)}} Q_{1,1,-2}^{(0,3)} Q_{-1,-1,2}^{(0,3)} \quad (3.33)$$

¹⁵ which should be the case for λ small since $Q_b^{(0,2)}$ starts at order $O(\lambda)$. For large λ , in principle this does not appear to be guaranteed from the gauge theory point of view. However, from string theory it appears always to be the case that the lowest winding modes become massless first.

where the subscripts in $Q^{(h,n)}$ denote the vortex numbers for each leg. Similarly, one can use the same argument before (2.31) to extract higher order terms in the effective action (2.31). The fact that we get (2.31) from divergences is guaranteed since vortex diagrams follow the rules of Feynman diagrams. It is also straightforward to work out the counterparts of (3.33) between λ_{2k} in string theory side and $Q^{(m,n)}$.

We note that on general grounds one expects that the free energy of the interacting theory can be written in terms of a matrix integral for U [21]

$$Z(\beta, \lambda) = \int dU e^{I(U)} \quad (3.34)$$

with $I(U)$ expanded in terms of all possible powers of $\text{tr}U^n$

$$\begin{aligned} I(U) = & Q^{(0)} + \sum_{n \neq 0} Q_n^{(2)} \text{tr}U^n \text{tr}U^{-n} + \sum_{\substack{nm \neq 0 \\ n+m+l=0}} Q_{nml}^{(3)} \text{tr}U^n \text{tr}U^m \text{tr}U^l \\ & + \sum_{\substack{n,m,l,p \neq 0 \\ n+m+l+p=0}} Q_{nmlp}^{(4)} \text{tr}U^n \text{tr}U^m \text{tr}U^l \text{tr}U^p + \dots \end{aligned} \quad (3.35)$$

where each $Q^{\dots(n)} = \sum_{h=0}^{\infty} Q^{\dots(h,n)}$ is a sum of contributions of diagrams of different genus h and \dots denotes windings of insertions. The vortex diagrams introduced earlier can be considered as the diagrammatical rules for computing (3.34). The effective action (2.31) then extracts the most important contribution near the Hagedorn temperature.

It is important to emphasize that our discussion above should also apply to strong coupling. $Q^{(n,m)}(\lambda)$, which are the basic building blocks of the vortex diagrams, can be defined non-perturbatively as follows. Since at each genus the number of Feynman diagrams grows with loops only as a power, we expect that $Q^{(n,m)}(\lambda)$ should have a finite radius of convergence in the complex λ plane. Once one obtains $Q^{(n,m)}(\lambda)$ near the origin, one can analytically continue them to strong coupling.

4. Conclusions and discussions

In this paper we extracted Hagedorn divergences to all string loop orders and showed that they can be resummed. The resummed amplitudes have the form of an integral over the potential (1.1) for the thermal scalar and smooth the divergences. We presented arguments both from a worldsheet approach and from Yang-Mills theories using AdS/CFT. In the double scaling limits (2.26), worldsheets with arbitrary number of thermal scalar insertions

become equally important, which is consistent with the expectation that the thermal scalar will condense and the spacetime background will shift.

The fact that one can obtain the thermal scalar potential to arbitrary higher orders by analyzing the local divergences in the thermal string phase is interesting. The potential would enable one to find other possible phases of the theory. The results also give an unambiguous prescription for computing the potential for the thermal scalar near the Hagedorn temperature from string amplitudes. The relation we found between vortex diagrams in Yang-Mills theory at finite temperature and degenerate limits of worldsheet Riemann surfaces is rather intriguing and worth investigating further.

Finally we note our strategy for extracting the thermal scalar potential should also be applicable to the tachyon condensation in a circle with anti-periodic boundary conditions (for a recent discussion see [39]).

Acknowledgments

We would like to thank I. Klebanov, A. Lawrence, J. McGreevy, J. Polchinski, S. Shenker, S. Wadia and B. Zwiebach for discussions and P. Talavera for collaboration at early stage of this work. This work is supported in part by Alfred P. Sloan Foundation, U.S. Department of Energy (D.O.E) OJI grant, funds provided by the U.S. Department of Energy (D.O.E) under cooperative research agreement #DF-FC02-94ER40818, and in part by National Science Foundation under Grant No. PHY05-51164.

Appendix A. Examples of (3.14)

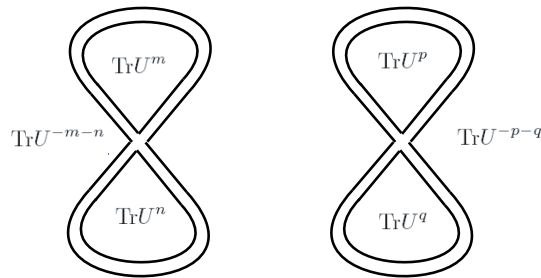


Fig. 10: Planar disconnected contributions to $\langle \text{Tr} M^4(\tau) \text{Tr} M^4(0) \rangle$

In this appendix we give some explicit examples on the use of equation (3.14) for calculating correlation functions between single trace operators. For definiteness we consider only bosonic operators, but the procedure is analogous for operators involving fermions. Consider the following simple example

$$\langle N\text{Tr}M^4(\tau)N\text{Tr}M^4(0) \rangle \quad (\text{A.1})$$

where M can be any of the bosonic modes in (3.1). The calculation of (A.1) amounts to drawing all possible double line diagrams. For example the disconnected planar contribution is given in fig. 10. From (3.12), each propagator carries an image number (or winding number), which should be summed over. Each face A carries a factor $\text{tr}U^{s_A}$. s_A is determined by choosing a direction for the propagators, and an orientation for the face, as explained below (3.16). fig. 10 therefore gives a contribution of the form

$$\frac{4}{N^2} \sum_{m,n,p,q=-\infty}^{\infty} G_s(-m\beta)G_s(-n\beta)G_s(-p\beta)G_s(-q\beta) \langle \text{Tr}U^m \text{Tr}U^n \text{Tr}U^{-m-n} \text{Tr}U^p \text{Tr}U^q \text{Tr}U^{-p-q} \rangle_U . \quad (\text{A.2})$$

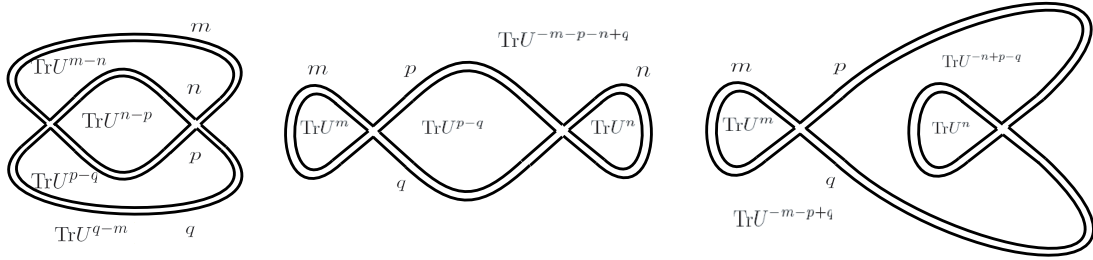


Fig. 11: Planar connected contributions to $\langle \text{Tr}M^4(\tau)\text{Tr}M^4(0) \rangle$

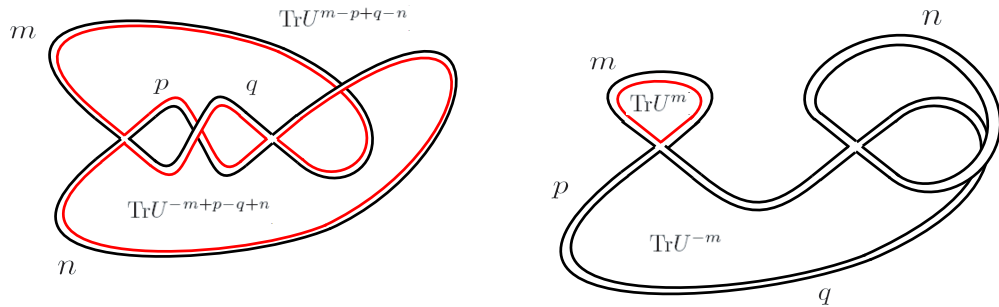


Fig. 12: Some non-planar (torus) connected contributions to $\langle \text{Tr}M^4(\tau)\text{Tr}M^4(0) \rangle$. For visualization purpose, the edge of one of the faces is drawn in red.

The connected planar contributions are given in fig. 11 with, for example, the first diagram given by

$$\frac{4}{N^2} \sum_{m,n,p,q=-\infty}^{\infty} G_s(\tau - m\beta)G_s(\tau - n\beta)G_s(\tau - p\beta)G_s(\tau - q\beta) \langle \text{Tr}U^{m-n}\text{Tr}U^{n-p}\text{Tr}U^{p-q}\text{Tr}U^{q-m} \rangle_U \quad (\text{A.3})$$

In fig. 12 we have also plotted some connected non-planar diagrams, with the first diagram given by

$$\frac{4}{N^2} \sum_{m,n,p,q=-\infty}^{\infty} G_s(\tau - m\beta)G_s(\tau - n\beta)G_s(\tau - p\beta)G_s(\tau - q\beta) \langle \text{Tr}U^{m-p+q-n}\text{Tr}U^{-m+p-q+n} \rangle_U \quad (\text{A.4})$$

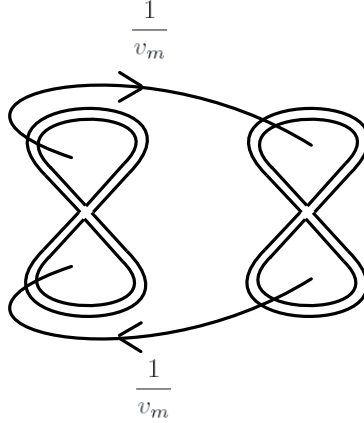


Fig. 13: Connected vortex diagram from disconnected double line diagram

Now let us consider the evaluation of the expectation values of traces of U in (A.2)-(A.4) using (3.20). At leading order in the large N expansion the expectation values give N^F , where F is the number of traces, times some product of Kronecker delta enforcing all exponents to be zero. In this case we recover the results of [37]. Higher order corrections in $1/N$ can be described graphically by inserting pairs of vortices on different faces of the diagrams and connecting them with the propagator $\frac{1}{v_b(\beta)}$. One should sum over all the possible ways of inserting pairs of vortices. Note that each vortex insertion gives a factor of $1/N$. Diagrams with disconnected parts connected by vortex propagators should be considered as connected as in fig. 13. Note that in terms of large N counting fig. 13 is of the same order as those in fig. 12 with no vortices.

Appendix B. Proof of (3.18)

In this appendix we prove equation (3.18). In the next subsection we discuss some elementary aspects of $U(N)$ group integrals. We then proceed to evaluate (3.8). Equation (3.18) is proved in the end.

B.1. Group integrals over $U(N)$

Consider the following integral over the unitary group $U(N)$

$$I = \frac{1}{V_N} \int dU \prod_{i=1}^k (\text{Tr} U^{a_i})^{b_i} \prod_{j=1}^s (\text{Tr} U^{-c_j})^{d_j} \quad (\text{B.1})$$

where a_i, b_i, c_i, d_i are positive integers and

$$D = \sum_{i=1}^k a_i b_i = \sum_{j=1}^s c_j d_j . \quad (\text{B.2})$$

V_N is the volume of $U(N)$.

Products of traces of U can be expanded in terms of characters of irreducible representations of $U(N)$, which are in one to one correspondence with irreducible representations of the symmetric group (see for example [40]),

$$\prod_{i=1}^k (\text{Tr} U^{a_i})^{b_i} = \sum_{\lambda} \chi_{\lambda}(a_i, b_i) \chi_{\lambda}(U) \quad (\text{B.3})$$

where λ labels the irreducible representations of the symmetric group S_D . $\chi_{\lambda}(a_i, b_i)$ is the character of the conjugacy class¹⁶ of S_D given by the set $\{(a_i, b_i)\}$ in the representation λ . $\chi_{\lambda}(U)$ is the character of U in the irreducible representation of $U(N)$ labelled by λ . Now by using the orthogonality property for characters we can write:

$$\begin{aligned} I &= \sum_{\lambda \lambda'} \chi_{\lambda}(a_i, b_i) \chi_{\lambda'}(c_i, d_i) \frac{1}{V_N} \int dU \chi_{\lambda}(U) \chi_{\lambda'}(U^{\dagger}) \\ &= \sum_{\lambda} \chi_{\lambda}(a_i, b_i) \chi_{\lambda}(c_i, d_i) . \end{aligned} \quad (\text{B.4})$$

¹⁶ Recall that two elements of S_D are conjugate if and only if they consist of the same number of disjoint cycles of the same lengths. Denote the number of cycles of length a_i by b_i then a conjugacy class in S_D is given by a set of k couples $\{(a_i, b_i)\}$ $i = 1, \dots, k$ such that $\sum_{i=1}^k a_i b_i = D$.

The evaluation of (B.4) can be divided into the following two cases:

1. If $D \leq N$, then the sum over λ can be evaluated giving [40]

$$I = \delta_{\{(a_i, b_i)\}, \{(c_i, d_i)\}} \sum_{\lambda} \chi_{\lambda}(a_i, b_i)^2 = \delta_{\{(a_i, b_i)\}, \{(c_i, d_i)\}} \prod_{i=1}^k a_i^{b_i} b_i! \quad (\text{B.5})$$

where the completeness of characters of the symmetric group S_D enforces the sets $\{(a_i, b_i)\}$ and $\{(c_i, d_i)\}$ to define the same conjugacy class in S_D , i.e., to be the same apart from reordering. This means that the integral is zero for $D < N$ unless for any factor of $\text{Tr}[U^a]^b$ in the integrand there is a corresponding factor of $\text{Tr}[U^{-a}]^b$.

2. If $D > N$ one needs to restrict the sum over the irreducible representations λ to the representations where $\chi_{\lambda}(U) \neq 0$, that we will indicate formally as $\lambda < N$. In this case the result is more complicated and we do not have a closed form expression. For the case in which the sets $\{(a_i, b_i)\}$ and $\{(c_i, d_i)\}$ are equal up to reordering one has

$$I = \sum_{\lambda < N} \chi_{\lambda}(a_i, b_i)^2 < \prod_{i=1}^k a_i^{b_i} b_i! . \quad (\text{B.6})$$

B.2. Partition function integrals

We now consider the evaluation of the free theory partition function (3.8). To warm up let us consider the following integral

$$\begin{aligned} \frac{1}{V_N} \int dU e^{z_1 \text{Tr} U \text{Tr} U^\dagger} &= \frac{1}{V_N} \int dU \sum_{p=0}^{\infty} \frac{1}{p!} (z_1 \text{Tr} U \text{Tr} U^\dagger)^p \\ &= \sum_{p=0}^N z_1^p + O(z_1^N) \\ &= \frac{1}{1 - z_1} + O(z_1^N) . \end{aligned} \quad (\text{B.7})$$

For $0 < z_1 < 1$ the corrections to the $N = \infty$ result are of order $O(z_1^N)$ and are therefore exponentially suppressed in N . In the more general case (3.8) (with $V_n(\beta) = z_n$) one can proceed exactly as above, writing

$$\begin{aligned} Z_0 &= \frac{1}{V_N} \int dU e^{I_0(U)} = \frac{1}{V_N} \int dU \exp \left(\sum_{n=1}^{\infty} \frac{z_n}{n} \text{Tr} U^n \text{Tr} U^{\dagger n} \right) \\ &= \frac{1}{V_N} \int dU \prod_{n=1}^{\infty} \left(\sum_{p_n=0}^{\infty} \frac{z_n^{p_n}}{p_n! n^{p_n}} (\text{Tr} U^n \text{Tr} U^{-n})^{p_n} \right) \\ &= \prod_{n=1}^{\infty} \frac{1}{1 - z_n} - C(N) \end{aligned} \quad (\text{B.8})$$

where $C(N)$ is given by

$$\begin{aligned}
C(N) &= \left[\prod_{n=1}^{\infty} \left(\sum_{p_n=0}^{\infty} z_n^{p_n} \right) - \frac{1}{V_N} \int dU \prod_{n=1}^{\infty} \left(\sum_{p_n=0}^{\infty} \frac{z_n^{p_n}}{p_n! n^{p_n}} (\text{Tr} U^n \text{Tr} U^{-n})^{p_n} \right) \right]_{\sum_n n p_n > N} \\
&< \left[\prod_{n=1}^{\infty} \left(\sum_{p_n=0}^{\infty} z_n^{p_n} \right) \right]_{\sum_n n p_n > N} \equiv D(N)
\end{aligned} \tag{B.9}$$

Note the the subscript in the above equation indicates that one should only sum over those p_n which satisfy $\sum_n n p_n > N$. $D(N)$ can be estimated as follows. Consider the expansion

$$\prod_{n=1}^{\infty} \frac{1}{1 - z_n t^n} = \sum_{n=0}^{\infty} a_n(z_1, z_2, \dots) t^n \tag{B.10}$$

where a_n are polynomials in the z_i with positive coefficients. Note that

$$D(N) = \sum_{n=N+1}^{\infty} a_n(z_1, z_2, \dots). \tag{B.11}$$

Define

$$z_* = \max(z_1, z_2^{\frac{1}{2}}, z_3^{\frac{1}{3}}, \dots, z_n^{\frac{1}{n}}, \dots) \tag{B.12}$$

Below T_H , we have $z_* < 1$. Then we have $0 < a_n(z_1, z_2, \dots) < a_n(z_*, z_*^2, z_*^3, \dots) = b_n z_*^n$ where the b_n 's are the coefficients of the series of $\prod_{m=1}^{\infty} \frac{1}{1 - z_*^m} = \sum_{n=0}^{\infty} b_n z_*^n$. This series has radius of convergence equal to 1 because the function has no singularities for $|z_*| < 1$. It then follows that for a given $\epsilon > 0$ there exists an $M(\epsilon)$ such that for $n > M(\epsilon)$ it is true that $b_n < (1 + \epsilon)^n$. Then for $\epsilon < \frac{1}{z_*} - 1$ and $N > M(\epsilon)$ the following holds:

$$C(N) < D(N) < \sum_{n=N+1}^{\infty} ((1 + \epsilon) z_*)^n = \frac{((1 + \epsilon) z_*)^{N+1}}{1 - (1 + \epsilon) z_*} \tag{B.13}$$

and therefore the corrections are exponentially small since $(1 + \epsilon) z_* < 1$.

To summarize we find that

$$Z_0 = \frac{1}{V_N} \int dU \exp \left(\sum_n \frac{z_n}{n} \text{Tr} U^n \text{Tr} U^{\dagger n} \right) = \prod_{n=1}^{\infty} \frac{1}{1 - z_n} - K e^{-Nc} \tag{B.14}$$

where $c = -\log(z_*) > 0$ and $K > 0$.

B.3. Correlation functions

Correlation functions (3.15)

$$\left\langle \prod_{i=1}^k (\text{Tr} U^{a_i})^{b_i} \prod_{j=1}^s (\text{Tr} U^{-c_j})^{d_j} \right\rangle_U = \frac{1}{Z_0} \int dU e^{I_0(U)} \prod_{i=1}^k (\text{Tr} U^{a_i})^{b_i} \prod_{j=1}^s (\text{Tr} U^{-c_j})^{d_j} \quad (\text{B.15})$$

where a_i, b_i, c_i, d_i are positive integers of order $O(N^0)$ can now be calculated easily using the technique above. Correlation functions of the form $\langle \prod_n (\text{Tr} U^{a_n} \text{Tr} U^{-a_n})^{b_n} \rangle_U$ are obtained by taking derivatives on Z_0 (B.14) with respect to $\frac{z_n}{n}$

$$\left\langle \prod_n (\text{Tr} U^{a_n} \text{Tr} U^{-a_n})^{b_n} \right\rangle = \frac{1}{Z_0} \prod_n n^{b_n} \frac{d^{b_n} Z_0}{dz_n^{b_n}}. \quad (\text{B.16})$$

If in (B.15) the $\{(a_i, b_i)\}$ are not matched with $\{(c_i, d_i)\}$ up to reordering, due to (B.5), the correlation function is zero up to nonperturbative corrections which are of order $(z^*)^N$. For example, $\langle \text{Tr} U^a \text{Tr} U^a \text{Tr} U^{-2a} \rangle_U$ is zero at any finite order in $\frac{1}{N^2}$ expansion unless a is zero.

The above results can be summarized by the following: the integrals can be evaluated by treating each $\text{Tr} U^n$ as an independent integration variable. More explicitly, replacing

$$\frac{1}{N} \text{Tr} U^n \rightarrow \phi_n, \quad \frac{1}{N} \text{Tr} U^{-n} \rightarrow \phi_{-n} = \phi_n^*, \quad \phi_0 = 1 \quad (\text{B.17})$$

then

$$\begin{aligned} & \left\langle \frac{1}{N} \text{Tr} U^{s_1} \frac{1}{N} \text{Tr} U^{s_2} \dots \frac{1}{N} \text{Tr} U^{s_F} \right\rangle_U \\ &= \frac{1}{Z_0} \int_{-\infty}^{\infty} \prod_{i=1}^{\infty} d\phi_i d\phi_i^* \phi_{s_1} \dots \phi_{s_F} \exp \left(-N^2 \sum_{n=1}^{\infty} \frac{1-z_n}{n} \phi_n \phi_n^* \right) + \text{nonperturbative in } N. \end{aligned} \quad (\text{B.18})$$

References

- [1] R. Hagedorn, *Nuovo Cim. Suppl.* **3**, 147 (1965).
- [2] K. Huang and S. Weinberg, *Phys. Rev. Lett.* **25**, 895 (1970).
- [3] S. Fubini and G. Veneziano, *Nuovo Cim. A* **64**, 811 (1969).
- [4] B. Sathiapalan, *Phys. Rev. D* **35**, 3277 (1987).
- [5] Y. I. Kogan, *JETP Lett.* **45**, 709 (1987) [*Pisma Zh. Eksp. Teor. Fiz.* **45**, 556 (1987)].
- [6] K. H. O'Brien and C. I. Tan, *Phys. Rev. D* **36**, 1184 (1987).
- [7] J. J. Atick and E. Witten, *Nucl. Phys. B* **310**, 291 (1988).
- [8] D. J. Gross, M. J. Perry and L. G. Yaffe, *Phys. Rev. D* **25**, 330 (1982).
- [9] B. Zwiebach, "A first course in string theory,"
- [10] J. Polchinski, "String theory. Vol. 1: An introduction to the bosonic string,"
- [11] H. Liu, "Fine structure of Hagedorn transitions," arXiv:hep-th/0408001.
- [12] L. Alvarez-Gaume, C. Gomez, H. Liu and S. Wadia, *Phys. Rev. D* **71**, 124023 (2005) [arXiv:hep-th/0502227].
- [13] J. Polchinski, *Commun. Math. Phys.* **104**, 37 (1986).
- [14] M. Kruczenski and A. Lawrence, *JHEP* **0607**, 031 (2006) [arXiv:hep-th/0508148].
- [15] S. W. Hawking and D. N. Page, *Commun. Math. Phys.* **87**, 577 (1983).
- [16] E. D'Hoker and D. H. Phong, *Rev. Mod. Phys.* **60**, 917 (1988).
- [17] A. A. Belavin and V. G. Knizhnik, *Sov. Phys. JETP* **64**, 214 (1986) [*Zh. Eksp. Teor. Fiz.* **91**, 364 (1986)].
- [18] J. L. F. Barbon and E. Rabinovici, *JHEP* **0203**, 057 (2002) [arXiv:hep-th/0112173].
J. L. F. Barbon and E. Rabinovici, arXiv:hep-th/0407236.
- [19] J. M. Maldacena, "The large N limit of superconformal field theories and supergravity," *Adv. Theor. Math. Phys.* **2**, 231 (1998) [*Int. J. Theor. Phys.* **38**, 1113 (1999)] [arXiv:hep-th/9711200].
S. S. Gubser, I. R. Klebanov and A. M. Polyakov, "Gauge theory correlators from non-critical string theory," *Phys. Lett. B* **428**, 105 (1998) [arXiv:hep-th/9802109].
E. Witten, "Anti-de Sitter space and holography," *Adv. Theor. Math. Phys.* **2**, 253 (1998) [arXiv:hep-th/9802150].
- [20] B. Sundborg, *Nucl. Phys. B* **573**, 349 (2000) [arXiv:hep-th/9908001].
- [21] O. Aharony, J. Marsano, S. Minwalla, K. Papadodimas and M. Van Raamsdonk, *Adv. Theor. Math. Phys.* **8**, 603 (2004) [arXiv:hep-th/0310285].
- [22] H. J. Schnitzer, *Nucl. Phys. B* **695**, 267 (2004) [arXiv:hep-th/0402219].
- [23] M. Spradlin and A. Volovich, *Nucl. Phys. B* **711**, 199 (2005) [arXiv:hep-th/0408178].
- [24] O. Aharony, J. Marsano, S. Minwalla, K. Papadodimas and M. Van Raamsdonk, *Phys. Rev. D* **71**, 125018 (2005) [arXiv:hep-th/0502149].
- [25] M. Gomez-Reino, S. G. Naculich and H. J. Schnitzer, *JHEP* **0507**, 055 (2005) [arXiv:hep-th/0504222].

- [26] P. Basu and S. R. Wadia, Phys. Rev. D **73**, 045022 (2006) [arXiv:hep-th/0506203].
- [27] K. Furuuchi, arXiv:hep-th/0608108.
- [28] L. Alvarez-Gaume, P. Basu, M. Marino and S. R. Wadia, arXiv:hep-th/0605041.
- [29] P. Basu, B. Ezhuthachan and S. R. Wadia, arXiv:hep-th/0610257.
- [30] T. K. Dey, S. Mukherji, S. Mukhopadhyay and S. Sarkar, arXiv:hep-th/0609038.
- [31] Y. Hikida, arXiv:hep-th/0610119.
- [32] T. Harmark and M. Orselli, Phys. Rev. D **74**, 126009 (2006) [arXiv:hep-th/0608115].
- [33] T. Harmark, K. R. Kristjansson and M. Orselli, arXiv:hep-th/0701088.
- [34] H. J. Schnitzer, arXiv:hep-th/0612099.
- [35] K. Papadodimas, H. H. Shieh and M. Van Raamsdonk, arXiv:hep-th/0612066.
- [36] G. 't Hooft, Nucl. Phys. B **72**, 461 (1974).
- [37] M. Brigante, G. Festuccia and H. Liu, Phys. Lett. B **638**, 538 (2006) [arXiv:hep-th/0509117].
- [38] D. J. Gross and I. R. Klebanov, Nucl. Phys. B **354**, 459 (1991);
I. R. Klebanov, “String Theory In Two-Dimensions,” arXiv:hep-th/9108019.
- [39] M. Dine, E. Gorbatov, I. R. Klebanov and M. Krasnitz, JHEP **0407**, 034 (2004) [arXiv:hep-th/0303076].
- [40] N. R. Constable and F. Larsen, “The rolling tachyon as a matrix model,” JHEP **0306**, 017 (2003) [arXiv:hep-th/0305177].